Copper–molybdenum–tungsten mineralization in granitoids around Kanchanpur–Thuni area, western Bundelkhand craton, central India

S. N. Rana*, P. Singh, S. K. Patle and V. P. Gaur

Geological Survey of India, Central Region, Bhopal 462 016, India

Highly altered granitoids in the western part of Bundelkhand craton around Kanchanpur and Thuni villages in Shivpuri district, Madhya Pradesh, India, are significantly associated with copper–molybdenum–tungsten mineralization which is manifested as stringers, blebs, clots and fine specks of chalcopyrite, pyrite, molybdenite and scheelite and as vein-fillings associated with hydrothermal alteration within the ore zone and adjacent host rocks. The cumulative strike length of the zone of mineralization (NW–SE) and associated alteration is around 3.5 km. Various mineral assemblages, viz. K-feldspar–biotite–chlorite, K-feldspar–sericite–chlorite and quartz–epidote–chlorite–sericite indicate intense hydrothermal alteration in the area. Analytical results have shown anomalous values for Cu (up to 1530 ppm), Mo (up to 4080 ppm) and W (up to 1449 ppm). Field observations and chemical analysis have been further supplemented by ore microscopic, petrographic, geochemical and EPMA studies to identify sulphide phases (of Fe, Cu and Mo) and scheelite. All the field and laboratory studies collectively indicate a probable hydrothermal origin of mineralization in the study area. The present study on Cu, Mo and W mineralization of economic grade in the western Bundelkhand craton has important implications for further metallogenic studies and mineral exploration in the area.

Keywords: Craton, granitoids, hydrothermal alteration, mineral assemblages, metallogenic studies.

BUNDELKHAND craton is among the five Archean cratons (Aravalli, Bastar, Dharwar and Singhbum cratons being the other four) in the peninsular region of India[1] (Figure 1 *a*), with an exposed area of around 26,000 km^2. It contains several large tracts of granitic rocks designated together as the Bundelkhand Granitoid Complex (BGC), which is overlain by the Palaeoproterozoic rocks of the Bijawar Group towards the southern margin, the Gwalior Group towards the northeastern margin and Mesoproterozoic rocks of the Vindhyan Supergroup towards the eastern, southern and western extremities[2–5] (Figure 1 *b*).

Without significant and economically viable mineral occurrences, BGC is generally considered barren as a whole[1]. However, notable occurrences of non-metallic and metallic minerals have been reported from various parts of BGC during the last few decades, important of which are pyrophyllite-diaspore[6], sporadic incidences of gold[7], molybdenite[8–10], basemetals[5] and iron[1]. Recently reported base metal (mainly Cu) and gold occurrences in BGC by Geological Survey of India (GSI) around Gwalior and Chhatarpur districts of Madhya Pradesh (MP), India, have opened newer avenues for further surface and subsurface exploration in the complex[5]. This communication presents features of a fresh finding of granitoid-hosted copper–molybdenum–tungsten (Cu–Mo–W) mineralization in western BGC.

The study area (parts of Kanchanpur and Thuni villages) is located about 65 km SE from the headquarters of Shivpuri district, MP. It lies in the western part of BGC, occupied by tonalite–trondhjemite–granodiorite gneiss (TTG), rhyolite, and variants of granite which in turn are traversed by quartz reefs. The TTG suite in the area occurred as enclaves of variable dimensions within younger rocks, viz. rhyolite and granites. A set-up of the volcano-sedimentary sequence was also present in the area, represented by rhyolitic and andesitic flows with calc-silicate interbands. Medium-grained granite was the most prominent rock type exposed in the area. Megascopically the rock was pink, pinkish-grey to grey in colour, medium-grained to coarse porphyritic. The porphyritic varieties contained phenocrysts of feldspars within a groundmass of quartz, feldspar and biotite. Thin veins of quartz were observed all over the area along major joints, viz. NE–SW and NW–SE (Figure 1 *c*).

Cu–Mo–W tungsten mineralization was associated with alkali feldspar granites traversed by numerous quartz veins (Figure 2 *a*). Mineralization was associated with hydrothermal alteration, as evident by K-feldspar alteration, chloritization, epidotization, silicification and oxidation (Figures 2 *b* and *c*). Indications of mineralization and associated hydrothermal alteration were well manifested as alteration haloes, malachite stains, brecciated quartz and calcite–epidote veins. The mineralization comprising Cu–Fe–Mo sulphides and scheelite occurred as fine to coarse disseminations, stringers, clots, blebs and veins fillings (Figure 2 *a*, *b* and *d*). The mineral alteration was mainly associated with sulphide phases and was insignificant in non-mineralized parts. Prominent wall-rock alterations and mineral assemblages observed in mineralized granitoids were: (i) K-feldspar–biotite–chlorite, (ii) K-feldspar–sericite–chlorite and (iii) quartz–epidote–chlorite–sericite representing potassic, phyllic and propylitic alteration respectively. Cross-cutting emplacement of mineralized veins was indicative of repeated fracturing and hydrothermal activity, as alteration features were most prominently observed along fractures in granitoids. The cumulative extension of mineralization was observed to be around 3.5 km in the NW–SE trend, indicating its emplacement along the NW–SE trending fracture system of BGC. Analytical results of the bedrock samples (Table 1) from the study area showed anomalous and economic content of Cu (755–1530 ppm), Mo (1597–4804 ppm) and W (123–1449 ppm) (Table 1).

Ore microscopic and Electron Probe Micro-analyzer (EPMA) studies at GSI, Faridabad revealed the presence of

*For correspondence. (e-mail: satya.rana@gsi.gov.in)

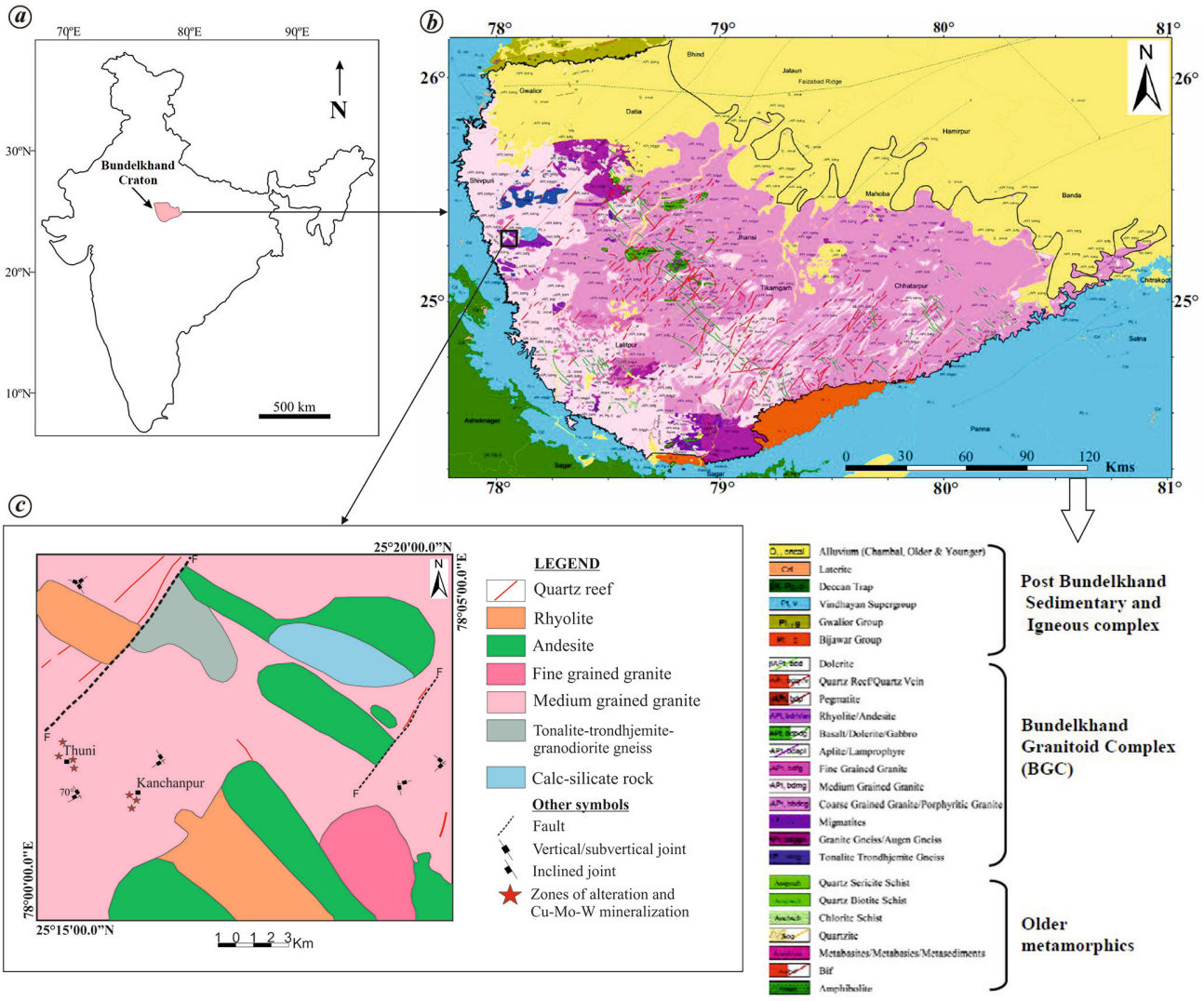

Figure 1. ***a***, Map of India showing the location of Bundelkhand craton. ***b***, Geological map of Bundelkhand Granitoid Complex with location of the study area. ***c***, Geological map covering parts of toposheet no. 54K/3 showing the zones of alteration and Cu–Mo–W mineralization around Kanchanpur and Thuni areas (modified after Shrivastava *et al*., unpublished).

pyrite, chalcopyrite, molybdenite and scheelite as important mineral phases (Table 2). Chalcopyrite was characterized by bright yellow colour occurring as anhedral grains (Figure 3 *a*) and also as fine specks and stringers. Molybdenite appeared as euhedral and subhedral flaky aggregates and discrete stringers (Figure 3 *b* and *c*). Scheelite occurred as stringers and isolated specks in association with other sulphides (Figure 3 *d*). Sulphide (Cu–Mo–Fe) and tungsten mineralization occured within the intergranular spaces, along quartz veins and fracture fillings.

Petrographic examination of the granitoids from the unaltered areas exhibited the mineral assemblage of quartz, K-feldspar and plagioclase as major phases, while hornblende and biotite were the minor minerals. Zircon, tourmaline, apatite, sphene and opaque occurred in accessory amounts. Texture appeared to be interlocking without any deformational fabric (Figure 4 *a*). Quartz was anhedral to subhedral and also appeared in fine-grained recrystallized form. K-feldspar occurred as large phenocrysts as well as smaller grains in the groundmass. Hornblende occurred in clusters, showing moderate birefringence with second-order interference colours, simple twins and symmetrical extinction. Biotite was pleochroic from light brown to dark brown in colour, with inclusions of euhedral apatite and zircon. Effects of hydrothermal alteration were well observed in the mineralized granitoids. Sericitization of the K-feldspars and pervasive alteration of hornblende and biotite to chlorite were the important features observed (Figures 4 *b* and *c*). Epidote was characterized by higher relief and higher order interference colour (Figure 4 *d*). Silicification, chloritization, epidotization and sericitization were significant alteration signatures which faded or became negligible in the granitoids away from the mineralized zones.

The major, trace and REE analyses (using XRF and ICPMS) of mineralized granitoids were carried out for their geochemical characterization (Table 3), which revealed

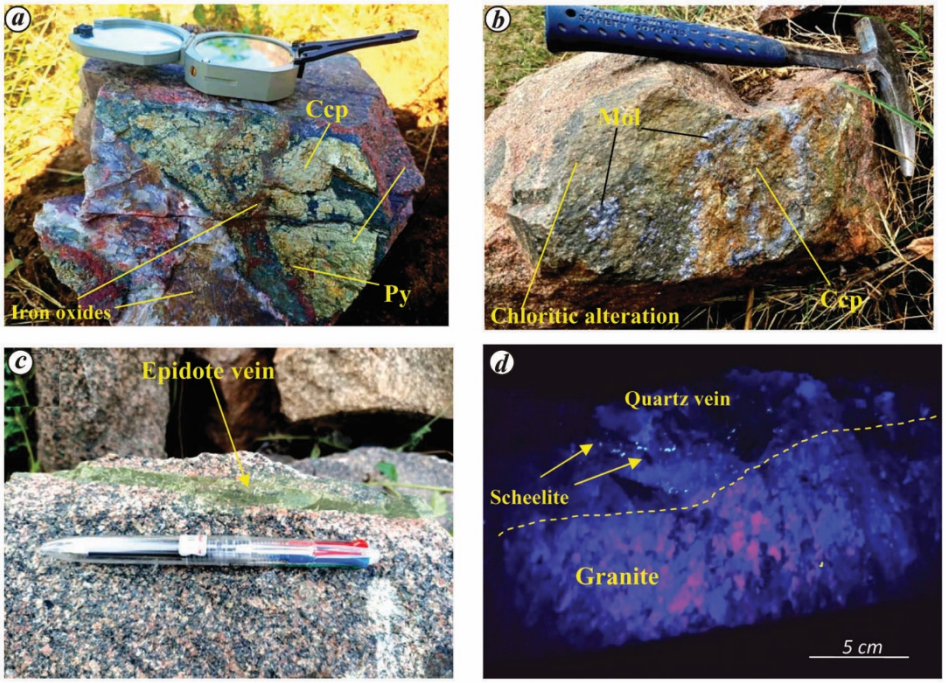

Figure 2. Field photographs showing mineralization and alteration around Thuni–Kanchanpur area. ***a***, Chalcopyrite (Ccp)–pyrite (Py) mineralization hosted in quartz vein intruded in granites. ***b***, Molybdenite (Mol)–chalcopyrite (Ccp) associated with chloritic alteration in granite. ***c***, Epidote vein in granite. ***d***, Fine dissemination of scheelite along quartz vein intruded into granite.

Table 1. Analytical results of bedrock samples collected from the study area

Sample no.	Rock type	Alteration	Cu (ppm)	Mo (ppm)	W (ppm)
BRS/NG/15	Granite with quartz veins	Potassic–chloritic alteration with epidote veins	65	4804	21.92
BRS/NG/16	Granite	Potassic alteration	55	78.71	5.44
BRS/NG/22	Granite with quartz veins	Potassic–chloritic alteration with epidote–calcite veins	755	1597	1449
BRS/NG/23	Granite with quartz veins	Potassic alteration with epidote veins	770	29.49	6.54
BRS/NG/45	Granite	Potassic alteration	270	25.8	123.83
BRS/NG/66	Granite with quartz veins	Potassic–chloritic alteration with epidote veins	1530	5.70	2.07

that they were characterized by moderate silica with SiO_2 content varying from 65.69 to 70.36 wt% with LOI (loss on ignition) ranging from 1.33 to 2.16 wt%. The Al_2O_3 concentration ranged between 12.19 and 15.07 wt%. Total alkali content ($Na_2O + K_2O$) was between 6.44 and 8.38 wt% (K_2O: 3.96–5.24 wt%, Na_2O: 2.48–3.34 wt%), confirming the dominancy of potash content over sodic content in these granitoids. Fe_2O_3 content (3.02–5.33 wt%) was greater compared to MgO (1.62–2.24 wt%). All the studied rocks belonged to the magnesian type of granite falling in metaluminous to peraluminous field[11] (Figure 5 *a*), with a slight negative trend when plotted in A/NK versus A/CNK classification diagram[12]. Trace element geochemistry suggested that fractional crystallization had played an important role during the evolution of these rocks. Rb, Sr and Zr showed strong negative relation with increasing silica, while positive relation was observed for Y, La and Ce. Granites and TTG from the study area showed enrichment of REE and LREE dominated over HREE concentration. The ∑LREE of granites varied from 214.7 to 311.13 ppm, while in TTG it varied from 153.68 to 190.48 ppm. A higher ratio of La/Lu in granite (188.76) and TTG (72.19) suggested strong fractionation of LREE during the evolution of these rocks. The chondrite normalized REE pattern showed that granitoids were highly enriched in LREEs, indicating a steep slope from La to Eu with negative Eu anomaly and almost a flat pattern for the HREEs[13] (Figure 5 *d*). The negative Eu of anomaly supports the fractionation of feldspar during the crystallization of the magma. Geochemical data of seven granitoids samples away from the mineralized areas were also analysed for geochemical characterization. The major oxide geochemistry showed that SiO_2 concentration varied from 70.6 to 73.78 wt%, Fe_2O_3 from 1.15 to 6.05 wt%, Al_2O_3 from 12.05 to 15.92 wt%, MgO from 0.2% to 2.89%, CaO from 0.36% to 4.25%, Na_2O from 2.72% to 3.94% and K_2O from 3.22% to 7.21%. Trace element and REE geochemistry of non-mineralized granitoids did not vary significantly compared

Table 2. Representative EPMA data (in wt%) of Cu–Mo–W-bearing quartz veins from the study area

Data point	1	2	3	4	5	6	7	8	9	10
Fe	46.418	29.939	1.558	29.756	0.129	46.273	0.137	0.14	0.222	0.127
Mn	0	0	0.027	0	0.011	0.012	0.011	0	0	0
Ti	0.025	0.002	0	0	0.014	0	0.027	0	0.048	0
Cu	0	34.227	0.194	33.759	0	0	0	0	0	0
Ni	0.05	0.021	0.022	0.023	0.003	0	0.015	0	0	0
Co	0.134	0.026	0	0	0	0.123	0	0.008	0	0.026
Zn	0	0.009	65.369	0.886	0.013	0.046	0	0	0	0
Te	0	0.029	0	0	0.184	0	0	0	0	0
V	0	0	0.021	0	0	0	0	0	0	0
Cr	0	0	0.016	0	0.02	0.005	0	0.003	0.014	0.034
S	53.374	34.915	33.225	34.85	39.378	53.195	40.5	0.091	40.122	40.887
Mo	0.792	0.391	0.538	0.478	58.022	0.747	60.894	0.641	60.656	60.64
Au	0.131	0.053	0	0.01	0.445	0	0.44	0	0.348	0.329
Ag	0.013	0	0	0	0.021	0	0.02	0	0.068	0.009
Cd	0	0	0.155	0	0	0.076	0	0	0	0
In	0.091	0	0.094	0	0.004	0	0	0	0	0
Sn	0	0.06	0	0.022	0.087	0.017	0.006	0	0.003	0.069
Sb	0.044	0	0	0	0	0	0	0	0.04	0.021
Ba	0	0.068	0	0.054	0	0	0.121	0.01	0.015	0.063
Pb	0	0	0	0	0	0	0	0	0	0
Bi	0.107	0.077	0.034	0.099	0	0.119	0	0	0	0
As	0.033	0.098	0	0.072	0	0	0.017	0	0	0
W	–	–	–	–	–	–	–	54.783	0.039	0.011
Comment	Pyrite	Chalcopyrite	Sphalerite	Chalcopyrite	Molybdenite	Pyrite	Molybdenite	Scheelite	Molybdenite	Molybdenite

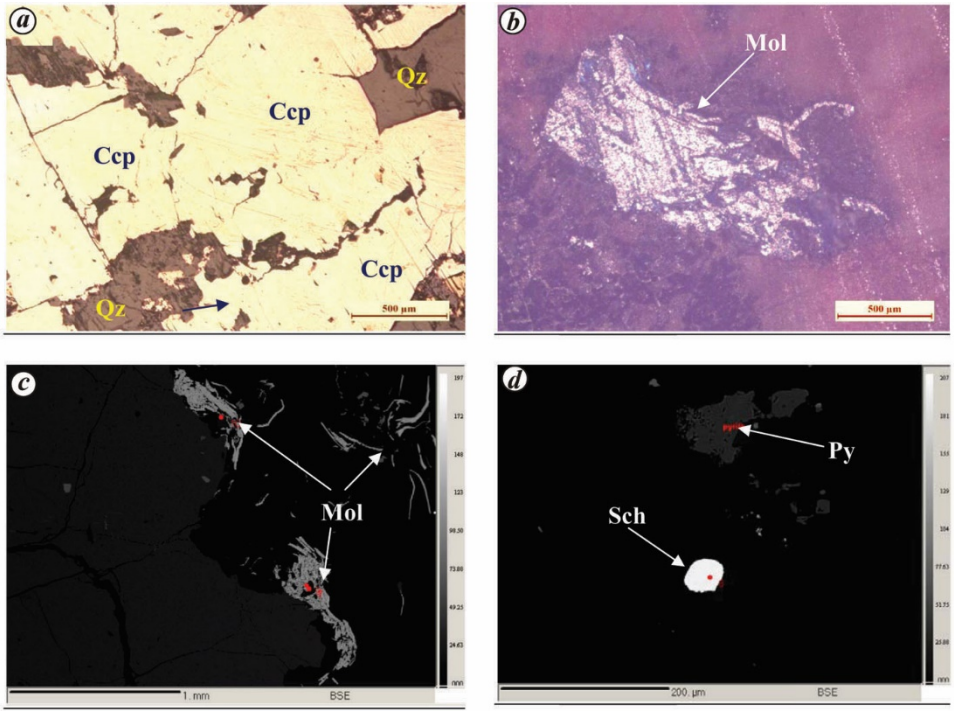

Figure 3. Photomicrographs and back scattered electron (BSE) images of sulphide–scheelite mineralization in study area. ***a***, ***b***, Photomicrographs showing (***a***) chalcopyrite (Ccp) hosted by quartz (Qz) vein and (***b***) molybdenite (Mol) hosted by medium-grained syenogranite. ***c***, ***d***, BSE image showing (***c***) molybdenite hosted by quartz vein and (***d***) scheelite (Sch) grain surrounded by pyrite (Py).

to the mineralized granitoids. In order to evaluate the tectonic setting of the studied rocks, samples were plotted in the standard discrimination diagrams which showed volcanic arc granite (VAG) to syn-COLG (collision granite) tectonic setting[14], with all the samples falling in the I-type granite field[15] (Figure 5 *b* and *c*).

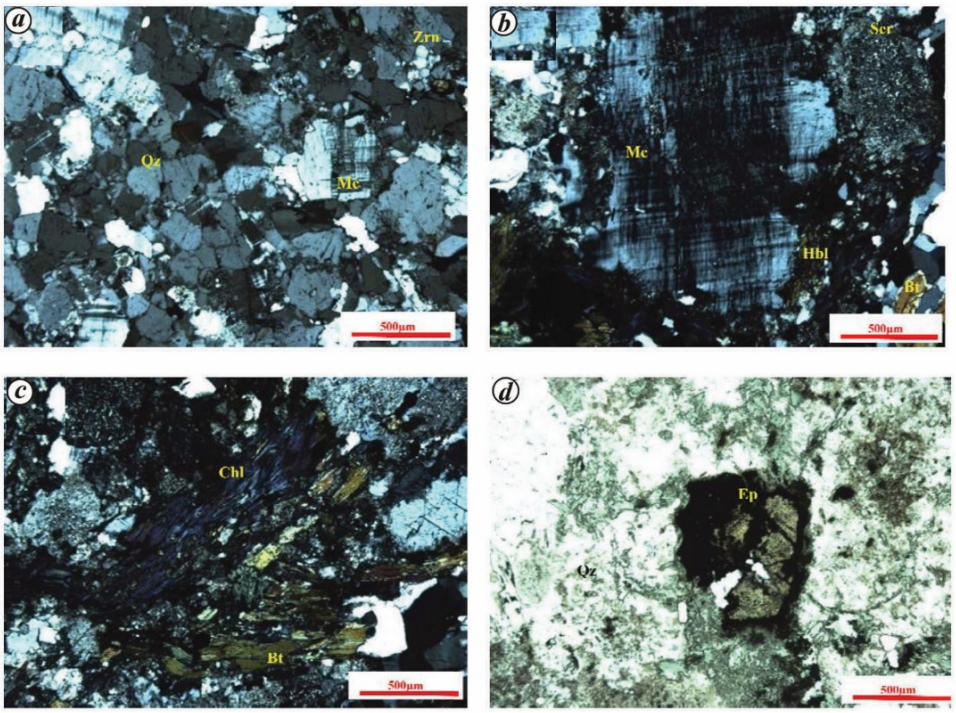

Figure 4. Photomicrographs displaying petrographic characters of granitoids from the study area. ***a***, Assemblage of K-feldspar, quartz and zircon (CPL view). ***b***, Phenocryst of microcline showing zoning associated with quartz, biotite and sericitized feldspar grain shown in the upper right corner (CPL view). ***c***, Chloritization of mafic phases (CPL view). ***d***, Epidote vein in association with quartz grain showing high relief (PPL view). CPL, Cross-polarized light; PPL, Plane polarized light.

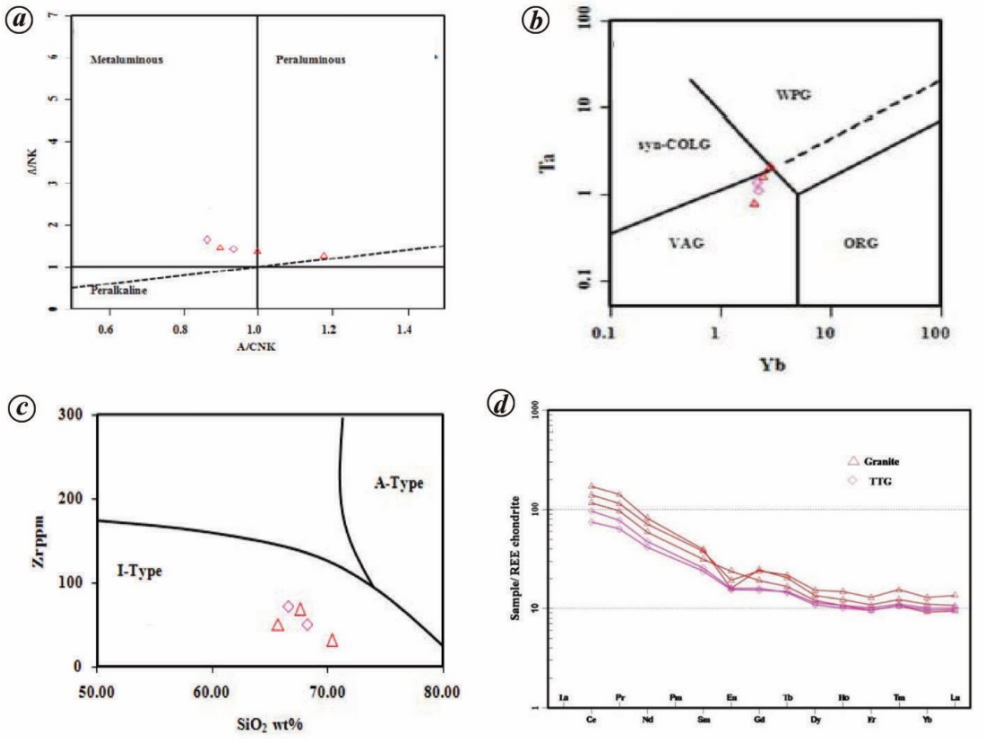

Figure 5. ***a***, A/NK–A/CNK diagram for granitoids from the study area (after Shand[12]). ***b***, Ta–Yb discrimination plot revealing that granitoids of the study area are of volcanic arc origin (after Pearce *et al.*[14]). ***c***, Zr versus SiO_2 binary diagram for granite (after Gunther *et al.*[15]). ***d***, Chondrite normalized REEs pattern for TTG and granites (after Nakamura[13]). Symbols are same as used in Figure 5 *d*.

Table 3. Representative petrochemical analysis of granitoids from the study area (values of oxides are in wt%, and of trace and REE in ppm)

Sample no./ oxides trace elements and REE	Samples from mineralized zones					Samples from non-mineralized areas						
	PS-1	PS-2	PS-3	PS-4	PS-5	PS-6	PS-7	PS-8	PS-9	PS-10	PS-11	PS-12
SiO_2	70.36	66.61	65.69	67.6	68.25	70.6	74.32	73.08	72.08	73.37	72.74	73.78
Al_2O_3	13.65	13.42	15.07	12.19	13.82	14.14	12.61	13.2	12.68	13.59	13.21	13.18
Fe_2O_3	3.02	5.33	3.22	5.28	3.87	2.17	1.15	1.99	1.44	1.38	1.45	1.78
CaO	0.47	4.1	2.28	2.87	2.86	1.02	0.6	0.81	0.57	0.86	0.94	0.63
MgO	1.62	2.24	2.17	2.43	1.68	0.49	0.19	0.59	0.27	0.2	0.3	0.27
Na_2O	3.09	3.32	3.34	2.48	3.42	3.51	3.03	2.85	2.87	3.17	3.16	3.98
K_2O	5.24	2.44	5.04	3.96	3.69	6.06	5.71	6.28	6.31	6.31	6.23	4.95
TiO_2	0.47	0.48	0.51	0.56	0.39	0.33	0.12	0.29	0.23	0.14	0.19	0.15
MnO	0.05	0.09	0.07	0.09	0.07	0.05	0.03	0.04	0.03	0.03	0.03	0.04
P_2O_5	0.17	0.16	0.19	0.23	0.13	0.07	0.03	0.12	0.04	0.04	0.07	0.04
LOI	1.47	1.33	2.16	2.06	1.46	0.56	0.47	0.72	0.37	0.81	1.61	0.63
Ga	19	20	19	18	19	17	14	18	15	18	20	21
Nb	12	13	12	15	12	13	7	23	12	32	53	18
Sc	8	13	11	14	10	12	12	15	nd	nd	10	8.4
Sr	162	357	367	249	315	150	70	153	101	87	85	84
V	43	63	46	74	47	10	10	10	10	10	10	12
Y	26	28	23	32	24	26	17	45	19	45	61	24
Zr	303	203	421	278	218	302	120	261	208	148	199	202
Be	2.49	1.65	3.87	1.71	1.74	2.26	3.93	1.86	nd	nd	2.01	1.96
Rb	198.71	91.67	154.28	132.81	127.73	204	206	315	246	458	493	163
La	87.19	35.09	57.56	66.35	47.65	98	184	33	153	57	56	3.4
Ce	147.67	64.69	100.74	120.91	83.55	168	222	74	173	114	101	9.8
Pr	15.79	7.08	10.77	12.75	8.67	17	36	10	25	11	11	0.9
Nd	51.27	26.17	37.41	44.88	29.82	58	118	47	80	38	37	3.2
Eu	1.23	1.19	1.84	1.48	1.22	1.22	1.83	3.23	1.65	1.10	0.81	0.13
Sm	7.98	4.79	6.38	7.69	5.21	9.27	17.81	11.00	11.32	6.02	6.37	0.81
Gd	6.80	4.20	5.28	6.54	4.39	7.50	14.41	10.65	9.70	5.12	5.33	0.71
Tb	0.95	0.69	0.78	1.01	0.68	0.98	1.94	1.95	1.35	0.70	0.78	0.13
Dy	4.64	3.90	4.16	5.22	3.69	4.40	10.03	11.16	7.16	3.61	4.09	0.89
Ho	0.86	0.75	0.75	1.03	0.70	0.69	1.89	2.15	1.34	0.69	0.72	0.20
Er	2.42	2.25	2.16	2.89	2.14	1.91	5.75	6.13	4.09	1.98	2.13	0.74
Tm	0.37	0.33	0.32	0.46	0.32	0.26	0.92	0.91	0.64	0.30	0.33	0.15
Yb	2.42	2.21	2.02	2.83	2.11	1.64	5.76	5.65	4.39	1.94	2.04	1.16
Lu	0.36	0.34	0.32	0.46	0.33	0.28	0.90	0.88	0.71	0.29	0.33	0.20

nd, Not detected.

Field observations, petrographic, geochemical, ore microscopic and EPMA studies established the occurrence of Cu–Mo–W mineralization in altered granitoids in the study area as stringers, blebs, clots and finely disseminated specks of chalcopyrite, pyrite, molybdenite and scheelite. Mineralization was prominently associated with different wall-rock alteration patterns, viz. potassic alteration (K-feldspar–biotite–chlorite), phyllic alteration (K-feldspar–sericite–chlorite) and propylitic alteration (quartz–epidote–chlorite–sericite). Geochemistry indicated that the Cu–Mo–W-bearing granitoids were highly potassic, metaluminous to peraluminous, moderately fractionated, volcanic arc-generated I-type granitoids. The emplacement of younger granites into older TTG suites of rocks provided paths for the circulation of hydrothermal fluid and leaching of K, Fe, Cu, Mo and W during the course of wall-rock alteration. Occurrence of Cu–Mo–W mineralization hosted by alkali feldspar granite and quartz veins over a considerable area, with highly anomalous values for Mo (up to 0.48%), W (up to 0.14%) and Cu (up to 0.15%) along with pervasive hydrothermal alteration of host rocks, fracture-controlled mineralization (coinciding with regional NW–SE trending fracture system of BGC) and dominantly metaluminous nature of granitoids collectively indicate a probable hydrothermal origin for mineralization in the study area.

Conflict of interest: The authors declare that there is no conflict of interest.

1. Basu, A. K., Geology of parts of the Bundelkhand granite massif, central India. *Rec. Geol. Surv. India*, 1986, **117**, 61–124.
2. Ramakrishnan, M. and Vaidyanadhan, R., *Geology of India*, Geological Society of India, Bangalore, 2010, vol. 1, pp. 249–260.
3. Kaur, P., Zeh, A. and Chaudhari, N., Characteristic of U–Pb–Hf isotope record of the 3.55 Ga felsic crust from the Bundelkhand Craton, northern India. *Precambrian Res*., 2014, **255**, 236–244.
4. Singh, S. P., Subramanyam, K. S. V., Manikyamba, C., Santosh, M., Rajanikanta Singh, M. and Chandan Kumar, B., Geochemical systematics of the Mauranipur–Babina greenstone belt, Bundelkhand

Craton, Central India: insights on Neoarchean mantle plume-arc accretion and crustal evolution. *Geosci. Front*., 2018, **9**, 769–788.
5. Gaur, V. P and Shahid, M., *Geology and Mineral Resources of Bundelkhand Granitoid Complex*, Special Publication, Geological Survey of India, Nagpur, 2021.
6. Sharma, R. P., Origin of the pyrophyllite–diaspore deposits of the Bundelkhand Complex, Central India. *Miner. Deposita*, 1979, **14**, 343–352.
7. Pati, J. K., Raju, S., Mamgain, V. D. and Shankar, R., Gold mineralisation in parts of Bundelkhand Granitoid Complex (BGC). *J. Geol. Soc. India*, 1997, **50**, 601–606.
8. Nim, S. P. and Hassan, S. S., Specialized thematic studies of Bundelkhand granitoids for appraisal of the mode of occurrence of molybdenum and associated mineralization, Rauli Kalyanpur area, Banda districts, UP. *Rec. Geol. Surv. India*, 1997, **129**, 142–144.
9. Shukla, R. and Singh, D. P., Specialized thematic studies of Bundelkhand granitoids for appraisal of the mode of occurrence of molybdenum and associated mineralization, Rauli Kalyanpur area, Banda districts, UP. *Rec. Geol. Surv. India*, 1997, **129**, 141–142.
10. Pati, J. K., Panigrahi, M. K. and Chakarborty, M., Granite-hosted molybdenite mineralization from Archean Bundelkhand craton–molybdenite characterization, host rock mineralogy, petrology, and fluid inclusion characteristics of Mo-bearing quartz. *J. Earth Syst. Sci*., 2014, **123**, 943–958.
11. Frost, B. R., Barnes, C. G., Collins, W. J., Arculus, R. J., Ellis, D. J. and Frost, C. D., A geochemical classification for granitic rocks. *J. Petrol.*, 2001, **42**(11), 2033–2048.
12. Shand, S. J., *The Eruptive Rocks*, John Willey, New York, 1943, 2nd edn, p. 488.
13. Nakamura, N., Determination of REE, Ba, Fe, Mg, Na and K in carbonaceous and ordinary chondrites. *Geochim. Cosmochim. Acta*, 1974, **38**(5), 757–775.
14. Pearce, J. A., Harris, N. B. W. and Tindle, A. G., Trace element discrimination diagrams for the tectonic interpretation of granitic rocks. *J. Petrol*., 1984, **25**, 956–983.
15. Gunther, J., Kleeman, M. and Twisted, D., The compositionally-zoned sheet-like granite pluton of the Bushveld complex: evidence bearing on the nature of A-type magmatism. *J. Petrol*., 1989, **30**, 1383–1414.

ACKNOWLEDGEMENTS. We thank Dr S. Raju, Director General, Geological Survey of India (GSI), Kolkata and Dr J. Rajeshwar (GSI Nagpur) for their encouragement to publish this work. We also thank V. V. Mugal (GSI, CR, Nagpur); S. Sarkar (GSI Bhopal), Sumit Kumar Ahirwar (GSI Bhopal) and Harman Mahanta (GSI Bhubaneswar) for technical advice and support. Constructive and valuable suggestions by the anonymous reviewers and editorial handling by Prof. N. V. Chalapthi Rao are deeply acknowledged.

Received 29 November 2022; revised accepted 12 June 2023

doi: 10.18520/cs/v125/i5/561-567